MATLAB Simscape Model of An Alkaline Electrolyser and Its Simulation with A Directly Coupled PV Module

David Martinez and Ramon Zamora*

Electrical and Electronic Engineering Department, Auckland University of Technology, Auckland 1010, New Zealand

(david.martinez@outlook.co.nz, ramon.zamora@aut.ac.nz)

*Corresponding Author; Dr. Ramon Zamora, Electrical and Electronic Engineering Department, Auckland University of Technology, Auckland 1010, New Zealand, Tel: +64-9-921-9999, ramon.zamora@aut.ac.nz

Received: 22.11.2017 Accepted:28.01.2018

Abstract- This paper discusses a MATLAB/Simulink/Simscape power system implementation of an alkaline electrolyser directly coupled to a photovoltaic module. Meteorological average daily irradiance and temperature data for a typical summer and winter day in Auckland, New Zealand, is used in a 15-hour simulation duration to show characteristic responses of the system. In addition to the steady state output, boundary conditions are applied to the referenced mathematical models to include the transient performance, governed by the photovoltaic module internal parameters. The simulation results show that the steady state output of the proposed implementation matches the general response of similar systems reported in previous published papers. Overall electrolyser efficiency of 68.48% for summer and 63.32% for winter is in accordance with results from the referenced studies.

Keywords- Alkaline electrolyser; Simscape; hydrogen; PV module; irradiance.

1. Introduction

Energy storage systems are considered the key factor to improve reliability and stability of renewable-energy-based electricity [1]. For intermittent renewable energy sources, such as solar and wind, energy storage not only provides a way to match generation and load profiles but also serves as an auxiliary source to deliver power when renewable sources are unavailable.

Due to its sustainable production, hydrogen energy storage can be considered as the most promising energy storage technology [2]–[5]. Like electricity, hydrogen can be produced from renewable or non-renewable sources, and can have a wide range of environmental impact. Among those classified as renewable, water electrolysis is considered the best mechanism for hydrogen production due to its high sustainability with low or no harmful emissions [6]–[8].

Using DC current, a water molecule can be broken into hydrogen and oxygen. This process occurs inside an electrolyser which consists of two electrodes and an electrolyte. Depending on characteristics of the electrolyte, three different types of electrolyser exist: alkaline, proton exchange membrane (PEM) and solid oxide (SOE) [2].

Due to its high maturity and economical costs, alkaline electrolysis is the most commonly used technology to produce hydrogen using water [9]. Even though the technology is already advanced, many challenges still exist, primarily in efficiencies, overall system design and range of operation. Simulation is essentially important to further analyse these issues.

In the last three decades, several mathematical models have been proposed describing the operation of the electrolyser [10]. Models developed empirically from demonstration projects have received most attention due to their accuracy to represent operation characteristics of real

devices. Specifically, the model in [11] has been used in many studies showing not only accuracy but high adaptability to describe various real electrolysers.

Among existing simulation platforms, MATLAB offers several benefits to model any type of systems with a growing community support [12]. Within the MATLAB/Simulink environment, Simscape allows the exploration of mathematical models in their own physical domain simplifying the understanding of their real behaviour and expanding the possibilities of interconnecting fundamental elements [13]–[15]. In the case of alkaline electrolysers, an electrical equivalent circuit has been proposed in [16], but the mathematical model interaction with the MATLAB/Simulink/Simscape circuit is not clearly defined.

This work will focus on the construction of a Simscape power system model of an alkaline electrolyser based on [11] and its evaluation by coupling a photovoltaic module for an average solar irradiance profile in Auckland, New Zealand. Initially, Simulink simscape models are constructed considering not only mathematical equations but also real data from several studies. Then, both elements are characterized to assess the validity of their response against expected outcome. Finally, a 15-hour simulation is run, using meteorological data from NIWA [17], to observe the electrical interaction of the elements.

2. Model Presentation and Simulink Block Construction

2.1. Alkaline Electrolyser

Water can only be split into hydrogen and oxygen when a minimum electrical voltage is applied. Ideally the cell voltage is equal to this minimum voltage, called reversible voltage, but due to irreversibility, the cell voltage is always higher [9].

The extra voltage present in the cell is called overvoltage and is composed of ohmic, activation and diffusion overvoltages. Ohmic overvoltage is the overvoltage due to overall resistance of all components of the electrical circuit, while the activation overvoltage is the overvoltage related to extra energy required to start the oxygen and hydrogen formation process in the electrodes [18]. Diffusion overvoltage only takes precedence at high current densities when the reaction changes from electronic transfer to matter transfer [19].

An empirical model involving ohmic and activation overvoltages proposed in [11] is expressed by Eq. (1). The model has six different parameters to characterize the logarithmic response of an electrolyser cell voltage in terms of current and temperature.

$$V = V_{rev} + \frac{r_1 + r_2 T}{A} I + slog\left(\left(t_1 + \frac{t_2}{T} + \frac{t_3}{T^2}\right)\frac{I}{A} + 1\right) \quad (1)$$

where: T is the temperature of the cell, A is the area of the electrodes, r_1 and r_2 are the ohmic overvoltage parameters, and t_1, t_2, t_3, and s are the activation overvoltage parameters.

V_{rev} is the reversible voltage of the cell and is temperature and pressure dependant with a value of 1.229 V at standard conditions (1 bar, 25 °C). For low temperature ranges of up to 100 ^{0}C, voltage variation is small and can be considered constant [11].

Production rate of hydrogen can be related to the input current using Faraday law. An empirical expression for the hydrogen production efficiency is called Faraday efficiency [11]. This relationship is summarized in Eq. (2).

$$\dot{n}H_2 = \left(\frac{(I/A)^2}{f_1 + (I/A)^2} f_2\right)\frac{I}{zF} \quad (2)$$

where: f_1 and f_2 are parameters related to Faraday efficiency, z is the number of electrons transferred in the reaction (2 electrons for water electrolysis), F is Faraday constant and $\dot{n}$ is the molar flow rate per second.

f_1 and f_2 are usually considered constant for the overall model. However, they vary with temperature [11]. The assumption of linear relation with temperature in [11] depends on the temperature range of operation. In this research, a linear expression only applies for f_1 whereas for f_2 a limit value must be set to guarantee a range value between 0 and 1. Using the experimental data shown in Table 1, a linear empirical expression is obtained for f_1 as shown in Eq. (3) and a quadratic for f_2 as shown in Eq. (4). Note that an extra point was added to f_2 at 0 °C to guarantee a limit value of 1.

$$f_1 = 2.5T + 50 \quad (3)$$
$$f_2 = 1 - 6.25\text{x}10^{-6}T \quad (4)$$

A unit conversion is needed for the flow rate in Eq. (2) to obtain a rate in kilograms rather than moles. This will facilitate comparisons in the result section. Using the volume of an ideal gas at standard conditions v_{std}, the volumetric flow rate and the mass flow rate is given by Eq. (5).

$$\dot{V} = \dot{n}v_{std} \rightarrow \dot{M} = \dot{V}c \quad (5)$$

where: v_{std}= 0:0224136 m^3/mol and c = 0.08988 kg/m^3.

Table 1. Electrolyser experimental data [11]

Temperature [°C]	f_1	f_2
0		1.00
40	150	0.99
80	250	0.96

2.2. Boundary Conditions for the Alkaline Electrolyser

Due to the presence of a logarithmic function in Eq. (1), a careful consideration is needed to avoid negative values that can produce unrealistic results. This is obvious at low levels of current where the model parameters cannot follow the electrolyser response properly.

Similarly, when input current is zero in Eq. (1), the electrolyser cell is equal to the reversible voltage and can potentially act as a voltage source feeding current to other elements of the electrical circuit. To avoid this situation, the mathematical element is disconnected from the circuit to block any current flow and to force the voltage to follow the external circuit.

Finally, production rate given by Eq. (2) only depends on the input current regardless of the voltage input. This is not accurate since water can only be divided into hydrogen and oxygen when the cell voltage is enough to provide the required activation energy. A special consideration is added to the model to produce hydrogen only if the cell voltage is greater than V_{rev}. The final set of boundary conditions can be expressed in equations (6) and (7).

Using Matlab/Simulink math blocks, equations (1)–(7) are constructed for each input and output. The electrolyser components in detail are shown in Figs. 1 and 2.

Simscape electrical interaction is added by utilizing voltage/current controlled sources blocks, voltage/current measurement blocks, and electrical connection ports from the power systems specialized technology toolbox.

For the electrolyser diagram shown in Fig. 3, the boundary condition of zero current was implemented with a diode between the mathematical block subsystem and the power systems blocks. Finally, a memory block was added to the electrolyser model to break the algebraic loop and to facilitate the convergence of the solution when other elements are connected.

$$V = \begin{cases} V_{rev} + \frac{r_1 + r_2 T}{A} I + s log\left(\left(t_1 + \frac{t_2}{T} + \frac{t_3}{T^2}\right)\frac{I}{A} + 1\right), & I > -A\left(t_1 + \frac{t_2}{T} + \frac{t_3}{T^2}\right)^{-1} \\ V_{rev} + \frac{r_1 + r_2 T}{A} I, & I \leq -A\left(t_1 + \frac{t_2}{T} + \frac{t_3}{T^2}\right)^{-1} \\ V_{outside}, & I = 0 \end{cases} \quad (6)$$

$$\dot{n}H_2 = \begin{cases} \left(\frac{(I/A)^2}{f_1 + (I/A)^2} f_2\right)\frac{I}{zF}, & V > V_{rev} \\ 0, & V \leq V_{rev} \end{cases} \quad (7)$$

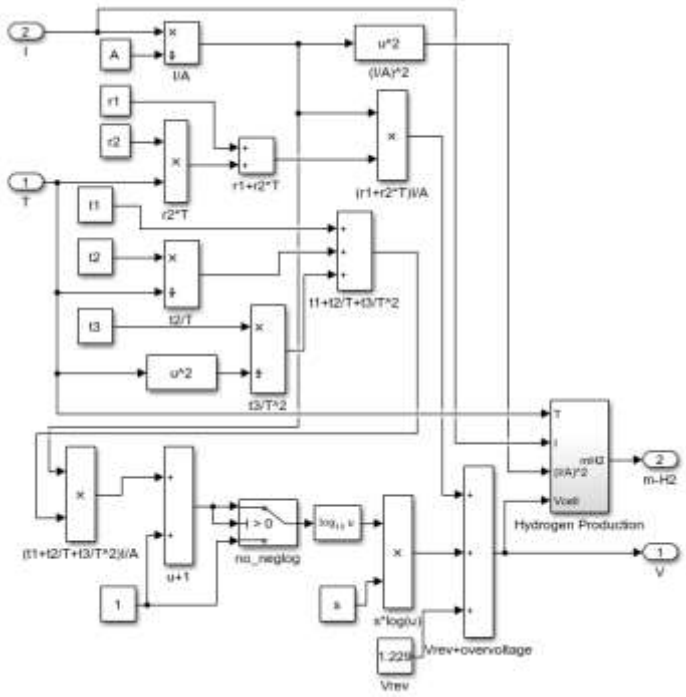

Fig. 1. Electrolyser block diagram.

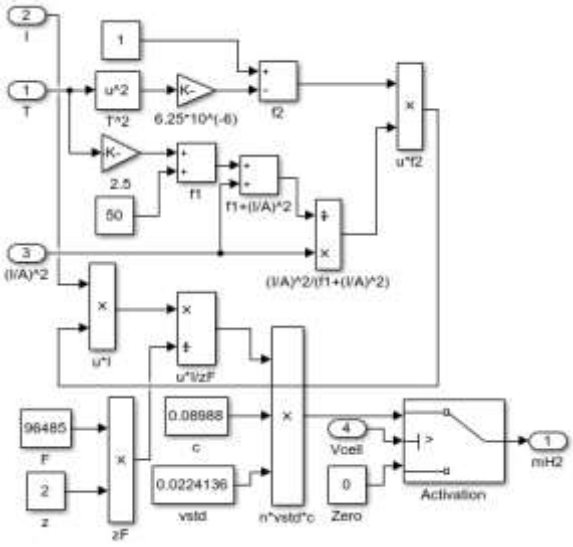

Fig. 2. Hydrogen production block diagram.

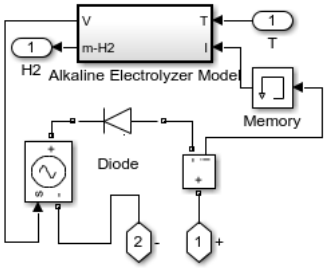

Fig. 3. Electrolyser simscape power systems integration.

2.3. PV Module

The semiconductor operation of a photovoltaic cell can be represented with the equivalent circuit shown in Fig. 4. The PV parameters are defined as follows: I_L is photo-generated current, I_d is diode current, I_p is current through parallel resistor, V_d is diode voltage, R_s is series resistance, and R_p is parallel resistance.

Based on Kirchhoff's current law (KCL), the output current is represented by Eq. (8).

$$I = I_L - I_d - I_p \tag{8}$$

where: $I_d = I_0\left(e^{\frac{qV_d}{nN_skT}} - 1\right)$ and $I_p = \frac{V_d}{R_p}$,

or

$$I = I_L - I_0\left(e^{\frac{qV_d}{nN_skT}} - 1\right) - \frac{V_d}{R_p} \tag{9}$$

where: I_0 is the reverse saturation current of the diode, T is the cell temperature, n is an ideality factor representing the type of technology, N_s is the number of cells connected in series, k is Boltzmann constant and q is the electron charge.

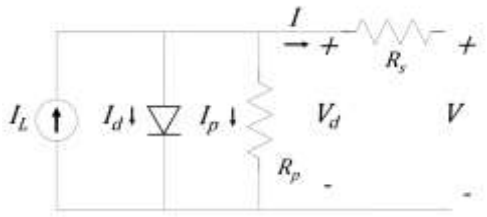

Fig. 4. PV module equivalent circuit.

The photo-generated current and the reverse saturation current are related to the physical parameters of a real PV module in [20] as expressed in equations (10)–(12).

$$I_L = \left(I_{sc} + \mu_{sc}(T - T_{ref})\right)\frac{G}{G_{ref}} \tag{10}$$

$$I_0 = I_{0-ref}\left(e^{\left(\frac{1}{T_{ref}} - \frac{1}{T}\right)\frac{q\varepsilon_g}{nk}}\right)\left(\frac{T}{T_{ref}}\right)^3 \tag{11}$$

$$I_{0-ref} = I_{sc}\left(e^{\frac{qV_{oc}}{nN_skT}} - 1\right) \tag{12}$$

where: I_{sc} is short circuit current, V_{oc} is open circuit voltage, G is irradiance input, G_{ref} is irradiance at STC = 1000 W/m^2, T_{ref} is temperature at STC = 25 °C, and ε_g is the material band gap energy, 1.12 eV for Si.

2.4. Boundary Condition for the PV Module

The output current of the equivalent circuit represented by Eq. (8) can generate negative values of current even if the photo generated current I_L is zero. However, this leads to an inaccurate result where the diode current I_d is still present even with no input energy. To avoid this situation a boundary condition is applied to the diode current in terms of the photo generated current as shown in Eq. (13).

$$I_d = \begin{cases} I_0\left(e^{\frac{qV_d}{nN_skT}} - 1\right), & I_L > 0 \\ 0, & I_L \le 0 \end{cases} \tag{13}$$

The equivalent circuit represented by equations (8) or (9) can be easily implemented in MATLAB/Simulink/Simscape with the power system specialized technology toolbox as shown in Figs. 5 and 6; The boundary condition for diode current is implemented with a simple Simulink switch. Simulink block details for equations (10)–(12) are not presented here since they have been presented in [20].

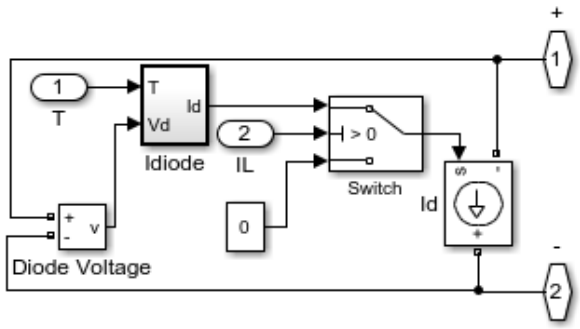

Fig. 5. PV diode current simscape power systems integration.

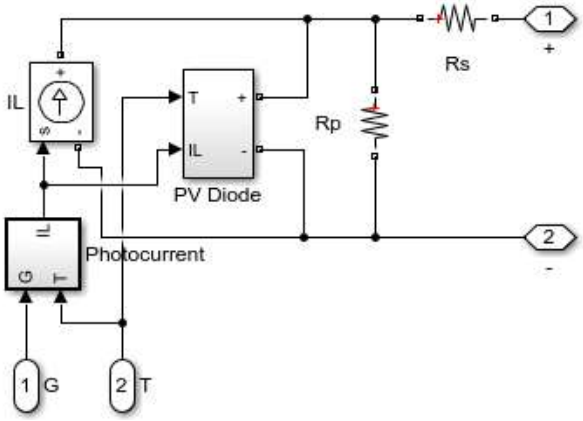

Fig. 6. PV module simscape power systems diagram.

3. Characterization of the Elements

To observe the response of each model to several temperatures, a variable input was introduced as a current source for the electrolyser and a variable resistor for the PV module. Ambient temperature values were selected according to average mean monthly minimum and maximums for Auckland: January/February average max. is 27 °C and July/August average min is 5 °C [21].

The parameters describing each model shown in Table 2 were tuned for the following equipment in the mentioned

studies: ELECTROCELL Micro Flow Cell [9] for the electrolyser and PWX 500 49W [20] for the PV module.

The I-V curves for the electrolyser and PV module are shown in Figs. 7 and 8 respectively. For both models the graphs match their mathematical representation. The impact of increasing the temperature in terms of voltage is positive for the electrolyser due to less cell overvoltage and negative for the PV module due to less power delivered.

Table 2. List of parameters for both models

Electrolyser	*Value*	*Units*	*PV Module*	*Value*	*Units*
A	0.01	m^2	I_{sc}	3.11	A
r_1	3.538550×10^{-4}	$\Omega\ m^2$	V_{oc}	21.8	V
r_2	-3.02150×10^{-6}	$\Omega\ m^2/^oC$	N_s	36	None
s	0.22396	V	n	1.3	None
t_1	5.13093	m^2/A	R_p	310.0248	Ω
t_2	-2.40447×10^2	$^oC\ m^2/A$	R_s	0.45	Ω
t_3	3.410251×10^3	$^oC^2\ m^2/A$			

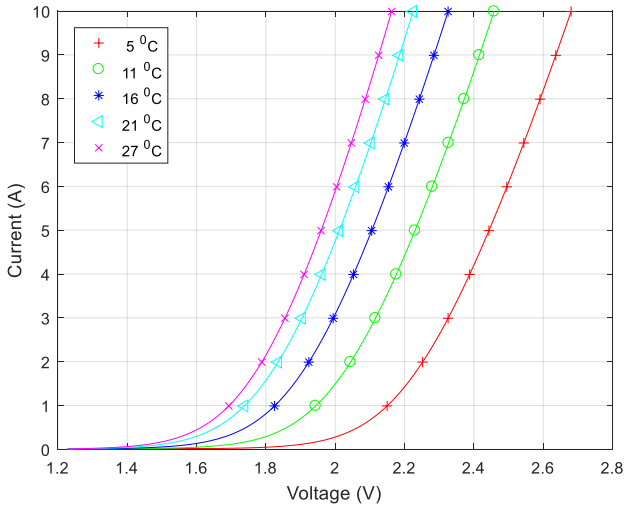

Fig. 7. Electrolyser I-V curve.

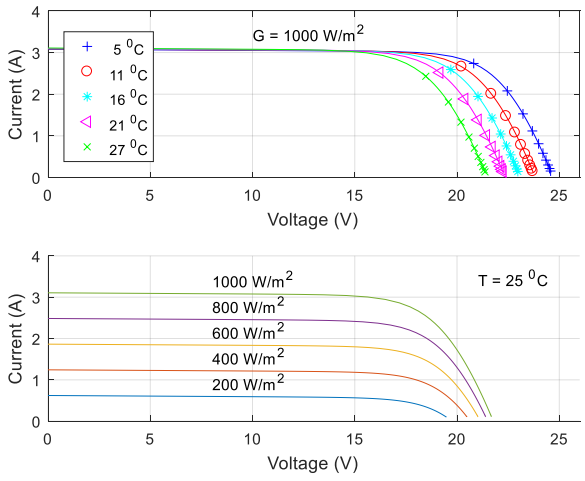

Fig. 8. PV module I-V curves.

4. System Simulation

To evaluate how the two electrical models interact with each other, the electrical ports of the two blocks were directly connected without implementing any voltage/current control or maximum power tracking, as shown in Fig. 9. Voltage and current are directly measured from the circuit while hydrogen production is obtained by adding an integrator to the hydrogen mass flow rate output of the electrolyser. The daily fluctuation of irradiance and temperature data are inputted from external csv files.

The months with maximum and minimum daily irradiation are evaluated in conjunction with average data for an entire year. Based on Auckland irradiance data from NIWA's SolarView [17], the irradiation values are 5.13 kWh/m^2 in January and 2.55 kWh/m^2 in June. The simulation is only performed during daylight hours considering January as the reference. The start time was selected to be close to dawn at 5 am and the end time was selected just after sunset at 8 pm, for a total of 15 hours of simulation time. The step size was arbitrary selected to be 60 seconds resulting in 901 data points.

Hourly average irradiance is given per hour for a total of only 15 points. To obtain the missing points representing 60 second intervals within each hour, an algorithm was created to generate a base sinusoidal curve of irradiance and then fit it to the given hourly average data. Working by hour intervals, the algorithm first calculates the average value of the base model, compares it to the average data and depending on the result, values are reduced or increased until the difference is below 0.01. A visualisation of the January data analysis is shown in Fig.

10. The error between the total cumulative values of the initial data and the fitted curve was only 0.04%, guarantying a correct input for the simulation.

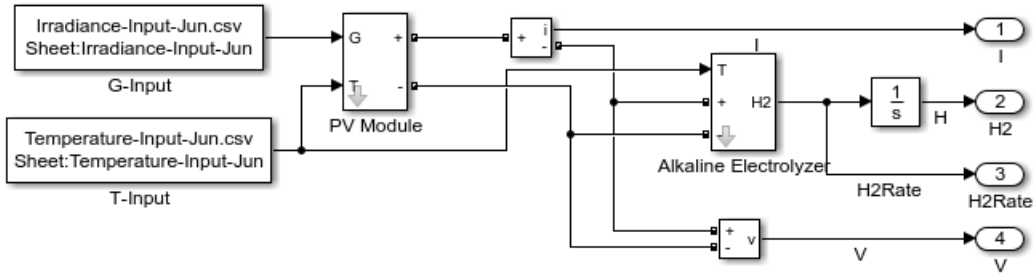

Fig. 9. System interconnection.

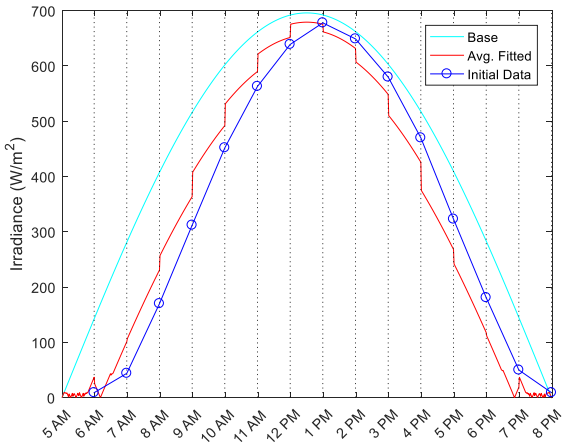

Fig. 10. Input irradiance data – January.

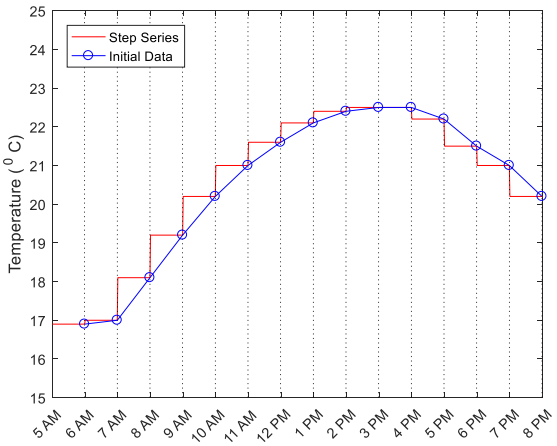

Fig. 11. Input Temperature data – January.

Temperature data from NIWA in [21] gives hourly average values for a total of 15 points. To obtain the missing points representing 60 second intervals within each hour, the algorithm generates a series of steps equal to the average temperature of the specific hour. A visualisation of the data analysis for January is shown Fig. 11. For average hourly temperature in a year, the mean value is calculated between the available data, which are summer maximum and winter minimum.

To assess the validity of the MATLAB/Simulink/simscape power systems model, four previous studies with similar simulation architecture were selected. Study A [22] ran a simulation using irradiance data for Miami USA, study B [23] used real devices for irradiance in Cairo Egypt, study C [24] used a real experimental setup in Algeria and study D [25] ran a simulation using irradiance data for Pamplona Spain. Unfortunately, due to the size difference of each system, the comparison mostly just involves the general trend of the output, following the shape of the curves for each variable analysed.

5. Results and Discussion

Since the voltage variation of the electrolyser cell for all given temperatures is much lower than the knee of the I-V curve of the PV module (Vrev + 1.5 V << Voc), the module acts as a current source proportional to the irradiance. This proportional relationship is shown in Fig. 12 with both irradiance and current curves superimposed for all evaluated cases. The compared studies also show the same responses where current follows the irradiance patterns.

The voltage curve in Fig. 13 shows a different pattern where two zones can be clearly identified. Steady state zone A is where the electrolyser is fully active and transient zone B is a startup/shutdown region where voltage fluctuation is predominant.

The shape of the output curves agrees with all four compared studies for the steady state zone A. However, the zone B characteristics cannot be compared since all referenced papers ignored the transient response.

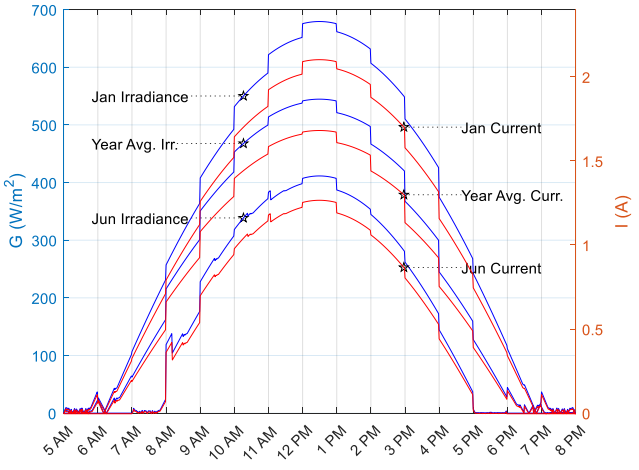

Fig. 12. Input Irradiance and output current.

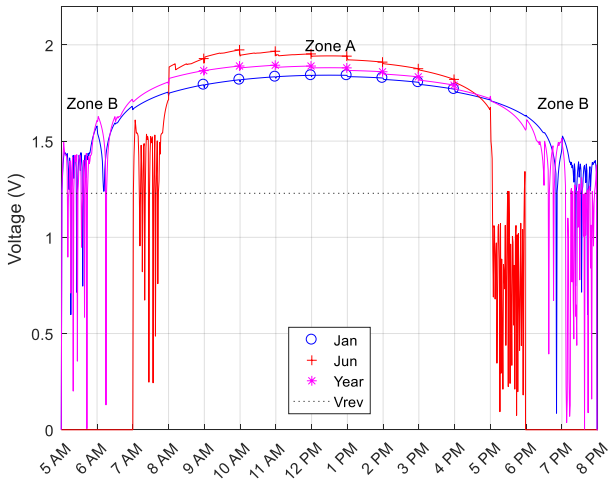

Fig. 13. Voltage curves.

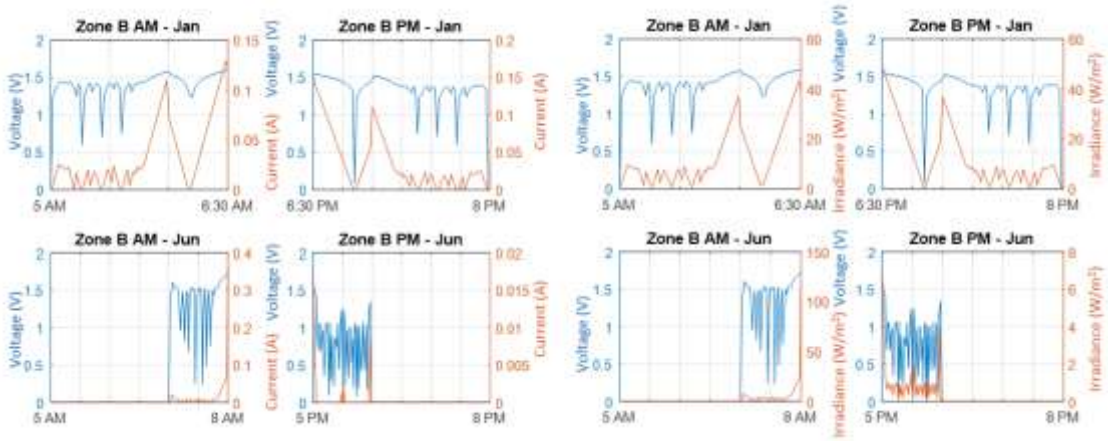

Fig. 14. Zone B region: voltage and current (left), voltage and irradiance (right).

To further assess the response of the transient zone B, a closer examination is performed by analysing the specific times of occurrence and the level of variation. By visual inspection, for January data, zone B finishes around 6:30 am and starts again at 6:30 pm. For June data, zone B finishes at 8 am and starts again at 5 pm. After a careful inspection of the data, with voltage superimposed with both irradiance and current shown in Fig. 14, the variation in voltage occurs in the PV module due to a low-level input of irradiance that is not high enough to generate current to the external circuit, dissipating through the PV module parallel resistance. The resulting voltage is then directly proportional to the irradiance and the internal parallel resistance of the PV module.

The amount of electrical energy inputted to the system can be found by calculating the area under the power curve. For the summer day, the total input energy was 26.1625 Wh and for the winter day 19.668 Wh. Based on Eq. (5), the amount of hydrogen produced by the single electrolyser cell was found to be 0.5856 grams in summer and 0.29 grams in winter which represents 19.3248 Wh and 9.57 Wh, respectively. The electrolyser efficiency is then calculated to be 68.48% and 63.32% for summer and winter, respectively. These values fall in the range of reported efficiency values in [2] and [18]. The energy and volume were calculated based on the hydrogen energy content of 120 MJ/kg or 33 kWh/kg and the volumetric density of 0.089 kg/m^3 [26], [27].

To allow a further comparison with the reference studies, instantaneous efficiency and flow rate was plotted in Fig. 15 for January, June and year average irradiance values. As expected from Eq. (2), the flow rate follows current. This general outcome matches the curves in the four reference studies.

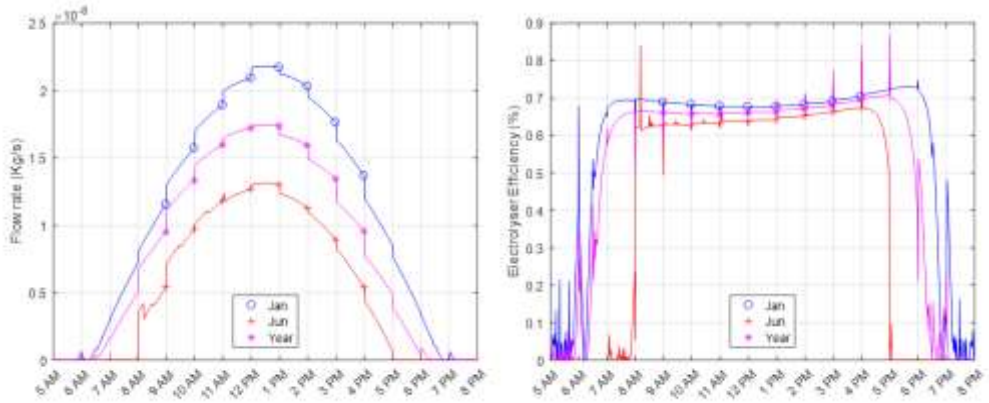

Fig. 15. Flow rate (left) and instantaneous efficiency (right).

6. Conclusions

A direct coupling of an alkaline electrolyser cell and a PV module was implemented in MATLAB/Simulink/Simscape power systems. Meteorological irradiance data from Auckland was used to simulate and verify the model. Boundary conditions were added to the referenced mathematical models to obtain an accurate transient response of the system. Voltage, flow rate and current steady state outputs matched previous studies while the transient response showed a direct relation to the PV internal parallel resistance. Overall electrolyser efficiency of 68.48% for summer and 63.32% for winter agrees with results provided in the referred published articles.

Further work is needed to add the thermal response of the model, storage alternatives and include other elements of the Simulink/Simscape family to allow a multi physical domain simulation.

References

[1] B. Zakeri and S. Syri, "Electrical energy storage systems: a comparative life cycle cost analysis", Renewable and Sustainable Energy Views, vol. 42, pp. 569-596, Ferbuary 2015.

[2] F. Zhang, P. Zhao, M. Niu, and J. Maddy, "The survey of key technologies in hydrogen energy storage", International Journal of Hydrogen Energy, vol. 41, pp. 14535-14552, September 2016.

[3] S. Dahbi, I. Mazozi, M. E. Ouariachi, A. Messaoudi, and A. Aziz, "Implementation of a Multi-control Architecture in a Photovoltaic/ Grid/ Electrolysis System for Usual Use and Clean Storage by Hydrogen Production", International Journal of Renewable Energy Research, vol. 7, no. 4, pp. 1825-1835, 2017.

[4] B. Mandal, A. Sirkar, A. Shau, P. De, and P. Ray, "Effects of Geometry of Electrodes and Pulsating DC Input on Water Splitting for Production of Hydrogen", International Journal of Renewable Energy Research, vol. 2, no. 1, pp. 99-102, 2012.

[5] Y. Allahvirdizadeh, M. Mohamadian, and M. HaghiFam, "Study of Energy Control Strategies for a Standalone PV/FC/UC Microgrid in a Remote Area", International Journal of Renewable Energy Research, vol. 7, no. 3, pp. 1495-1508, 2017.

[6] O. Bilgin, "Evaluation of hydrogen energy production of mining waste waters and pools", 4th International Conference on Renewable Energy Research and Applications, Palermo, pp. 557-561, November 2015.

[7] S. Kaya, B. Öztürk, and H. Aykaç, "Hydrogen Production from Renewable Source: Biogas", International Conference on Renewable Energy Research and Applications, Madrid, pp. 633-637, October 2013.

[8] K. Koiwa, R. Takahashi, and J. Tamura, "A Study of Hydrogen Production in Stand-alone Wind Farm", 2012 International Conference on Renewable Energy Research and Applications, Nagasaki, pp. 1-6, November 2012.

[9] E. Amores, J. Rodriguez, and C. Carreras, "Influence of operation parameters in the modelling of alkaline water electrolysers for hydrogen production", International Journal of Hydrogen Energy, vol. 39, pp. 13063-13078, 2014.

[10] P. Oliviera, C. Bourasseaua, and B. Bouamamab, "Low-temperature electrolysis system modelling: A review", Renewable and Sustainable Energy Reviews, vol 78, pp. 280-300, 2017.

[11] O. Ulleberg, "Modeling of advanced alkaline electrolyzers: a system simulation approach", International Journal of Hydrogen Energy, vol. 28, pp. 21-33, 2003.

[12] MathWorks, "Matlab", [Online]. Available: https://www.mathworks.com/products/matlab/features.html. [Accessed: 20-Nov-2017].

[13] MathWorks, "Simscape: Model and simulate multidomain physical systems", [Online]. Available: https://www.mathworks.com/products/simscape.html. [Accessed: 20-Nov-2017].

[14] M. R. Rashel, A. Albino, M Tlemcani, and T. C. F. Goncalves, "MATLAB Simulink modelling of photovoltaic cells for understanding shadow effect", 5th International Conference on Renewable Energy Research and Applications, Birmingham, pp.747-750, November 2016.

[15] K. Jazayeri, S. Uysal, and M. Jazayeri, "MATLAB/simulink based simulation of solar incidence angle and the sun's position in the sky with respect to observation points on the Earth", International Conference on Renewable Energy Research and Applications, Madrid, pp.173-177, October 2013.

[16] C. Henao, K. Agbossou, M. Hammoudi, Y. Dubé, and A. Cardenas, "Simulation tool based on a physics model and an electrical analogy for an alkaline electrolyser", Journal of Power Sources, vol. 250, pp. 58-67, 2014.

[17] The National Institute of Water and Atmospheric Research, "SolarView", [Online]. Available: https://solarview.niwa.co.nz/. [Accessed: 20-Nov-2017].

[18] K. Zeng and D. Zhang, "Recent progress in alkaline water electrolysis for hydrogen production and applications", Progress in Energy and Combustion Science, vol. 36, pp. 307-326, 2010.

[19] P. Oliviera, C. Bourasseaua and B. Bouamamab, "Low-temperature electrolysis system modelling: A review", Renewable and Sustainable Energy Reviews, vol 78, pp. 280-300, 2017.

[20] H. Bellia, R. Youcef, and M. Fatima, "A detailed modeling of photovoltaic module using MATLAB", NRIAG Journal of Astronomy and Geophysics, vol. 3, pp. 53-61, 2014.

[21] P.R. Chappel, "The Climate and Weather of Auckland, 2nd Edition" NIWA Science and technology series, Num. 60, pp. 23, [Online]. Available: https://www.niwa.co.nz/static/Auckland%20Climate WEB.pdf. [Accessed: 10-Nov-2017].

[22] A. Khalilnejad, A. Abbaspour, and A.I. Sarwat, "Multi-level optimization approach for directly coupled photovoltaic-electrolyser system", International Journal of Hydrogen Energy, vol. 41, pp. 11884-11894, 2016.

[23] G.E. Ahmad and E.T. El Shenawy, "Optimized photovoltiac system for hydrogen production", Renewable Energy, vol. 31, pp. 1043-1054, 2006.

[24] A. Djafour, M. Matoug, H. Bouras, B. Bouchekima, M.S. Aida, and B. Azoui, "Photovoltaic-assisted alkaline water electrolysis: Basic principles", International Journal of Hydrogen Energy, vol. 36, pp. 4117-4124, 2011.

[25] A. Ursua, I. S. Martin, E. L. Barrios, and P. Sanchis, "Stand-alone operation of an alkaline water electrolyser fed by wind and photovoltaic systems", International Journal of Hydrogen Energy, Vol. 38, pp. 14952-14967, 2013.

[26] K. Lu, Materials in Energy Conversion, Harvesting, and Storage, Hoboken, New Jersey: John Wiley & Sons, Inc. 2014, pp. 387.

[27] Universal Industrial Gases, Inc., "Unit Conversion Data for Hydrogen", [Online]. Available: http://www.uigi.com/h2_conv.html. [Accessed: 15-Nov-2017].